

1995/2/1345

Differenced Range Versus Integrated Doppler (DRVID) Ionospheric Analysis of Metric Tracking in the Tracking and Data Relay Satellite System (TDRSS)*

M. S. Radomski
Computer Sciences Corporation
Lanham-Seabrook, Maryland, USA 20706

C. E. Doll
National Aeronautics and Space Administration
Goddard Space Flight Center
Greenbelt, Maryland, USA 20771

Abstract

The Differenced Range (DR) Versus Integrated Doppler (ID) (DRVID) method exploits the opposition of high-frequency signal versus phase retardation by plasma media to obtain information about the plasma's corruption of simultaneous range and Doppler spacecraft tracking measurements. Thus, DR Plus ID (DRPID) is an observable independent of plasma refraction, while actual DRVID (DR minus ID) measures the time variation of the path electron content independently of spacecraft motion.

The DRVID principle has been known since 1961. It has been used to observe interplanetary plasmas, is implemented in Deep Space Network tracking hardware, and has recently been applied to single-frequency Global Positioning System user navigation. This paper discusses exploration at the Goddard Space Flight Center (GSFC) Flight Dynamics Division (FDD) of DRVID synthesized from simultaneous two-way range and Doppler tracking for low Earth-orbiting missions supported by the Tracking and Data Relay Satellite System (TDRSS).

The paper presents comparisons of actual DR and ID residuals and relates those comparisons to predictions of the Bent model. The complications due to the pilot tone influence on relayed Doppler measurements are considered. Further use of DRVID to evaluate ionospheric models is discussed, as is use of DRPID in reducing dependence on ionospheric modeling in orbit determination.

Introduction

This paper describes preliminary investigations of the Differenced Range (DR) Versus Integrated Doppler (ID) (DRVID) technique. DRVID uses the bandwidth of the coherent ranging signal to extract information about ionospheric delays from the comparison of simultaneous range and nondestruct Doppler observations, much as dual-frequency tracking compares two range or two Doppler observations. The idea is not new (Reference 1), but its application in the Goddard Space Flight Center (GSFC) Flight Dynamics Division (FDD) is. This investigation explores the quality and other properties of DRVID comparisons made using Tracking and Data Relay Satellite (TDRS) System (TDRSS) and Ground Network (GN) tracking data available at the GSFC Flight Dynamics Facility (FDF).

The paper is organized in sections that describe, respectively, the physical basis of DRVID, the analysis techniques, the results, and the conclusions of the investigation.

* This work was supported by the National Aeronautics and Space Administration (NASA)/Goddard Space Flight Center (GSFC), Greenbelt, Maryland, under Contract NAS 5-31500.

DRVID Background

The TDRSS or Unified S-Band (USB) two-way range observation is given by

$$R = \frac{1}{2}[R_L + I_L + T_L + D_L + E_L] \quad (1)$$

where

- R_L = long path length, i.e., the round-trip distance to the user (a spacecraft or a ground transponder of the Bilateral Ranging Transponder System (BRTS)) and back via a relaying TDRS (if using TDRSS).
- I_L, T_L, D_L = respective biasing effects of ionospheric, tropospheric, and residual transponder delays on signal propagation. D_L is constant during a tracking contact; any actual time variation in system delays is classified as belonging to E_L , below.
- E_L = effect of other measurement errors, such as extraction error and noise (including unbiased effects of ionospheric scintillation).
- R = total observation obtained by multiplying a measured round-trip time by the velocity of light, dividing by 2, and subtracting nominal user-transponder delay effects.

Successive range measurements can be differenced to synthesize the differenced range (DR)

$$DR = \Delta R \quad (2)$$

where Δ in Equation (2) and throughout this paper signifies differencing across the Doppler count interval corresponding to a contemporaneous Doppler observation.

Coherent nondestruct two-way Doppler observations measure finite differences of R_L by comparing the number of carrier wave fronts arriving in a Doppler count interval, ΔT , with the number transmitted in the same time span. If the Integrated Doppler (ID) is defined as

$$ID = -\frac{c \Delta T}{2A} D \quad (3)$$

where c is the velocity of light, A is the user-transmit frequency, D is the nondestruct Doppler observation, and ΔT is the Doppler count interval; then ID is a differenced observation

$$ID = \Delta r \quad (4)$$

of the phase-measured range

$$r = \frac{1}{2}[R_L - I_L + T_L + D_L + e_L + b(R_S - I_S + T_S + D_S + e_S)] + C_r \quad (5)$$

The quantities on the right-hand side of Equation (5) are defined as follows:

- The constant C_r is arbitrary, because r can only be defined by partial summation of Δr ; summed integrated Doppler (SID) observations measure r within a constant.
- The quantity D_L is the transponder phase delay effect (a constant, by definition, so that $\Delta D_L = 0$). In principle, this may differ from D_L in Equation (1) due to frequency dependence in the transponder delays. Any difference is time independent and is subsumed into the integration constant C_r .
- The error e_L is the phase-measurement error, differing from E_L because the Doppler extraction hardware is distinct from the range extraction hardware. The noise components within e_L and E_L are presumed independent.
- The quantities subscripted S correspond to those subscripted L but apply to the short path, or the return-link pilot round-trip loop of TDRSS observations rather than to the long relay round-trip. The short path goes from the receiving terminal to the TDRS and directly back, arriving simultaneously with the relayed signal. These quantities appear because the frequency translations applied to the signal by the relay are derived from the Doppler-shifted pilot tone broadcast by the receiving station.

- The quantity b is the ratio of the pilot frequency, B , to A . This ratio, constant for any given tracking contact, is about 5 for S-band single-access (SA) observations, about -1 for multiple-access (MA) observations, and 0 for non-TDRSS observations.

The negative sign before I_L and I_S in Equation (5) is a consequence of the inverse-square frequency dependence of the signal delays caused by the free-electron plasma of the ionosphere. This is in contrast to the nearly frequency-independent delays T_L and T_S caused by the bound electrons of the neutral troposphere. Because the frequencies of the links between the TDRS and the ground terminal are K-band (11 to 15 gigahertz), I_S is negligible compared with I_L , and the latter is dominated by the contribution of the S-band legs connecting the user to the TDRS.

Ground Network (GN)

For nonrelay tracking, the pilot term is absent. It is then possible to synthesize from simultaneous range and Doppler tracking the two data types (setting $b=0$):

$$DRPID \equiv \frac{1}{2}(DR + ID) = \frac{1}{2} \Delta [R_L + T_L + \frac{1}{2}(e_L + E_L)] \quad (6)$$

$$DRVID \equiv \frac{1}{2}(DR - ID) = \frac{1}{2} \Delta [I_L + \frac{1}{2}(E_L - e_L)] \quad (7)$$

The first of these is ionospherically unbiased, and the second is spacecraft independent. Note that the DRPID measurement set is equivalent to the measurement set obtained by calculating ΔI_L from Equation (7) and applying it to either DR or ID.

The DRPID dataset may be free of ionospheric bias but otherwise combines the worst features of the range and Doppler datasets. It has the noise of the range differences, yet shares with the Doppler data their lack of range zero-set information. The former problem can be ameliorated by summing the DRPID data, which filters the noise. This summed DRPID data (SDRPID) has about half as much noise as the original range data but still lacks zero-set information for each pass. This is crucial for orbit determination of a geosynchronous spacecraft, such as a TDRS, which requires unbiased range information to determine the east-west position. For a low Earth-orbiting (LEO) spacecraft, the necessity of solving for a range bias for each pass is not necessarily a heavy burden.

Orbit determination using the SDRPID data, discarding the SDRVID, avoids ionospheric error but may increase total error (see the above paragraph). It has been suggested (Reference 2) to reuse the original low-noise, approximately ionospherically corrected Doppler dataset together with SDRPID. This makes sense if the original Doppler frequencies are not summed. The white frequency-noise ionospheric error model implicit in this Doppler treatment corresponds to a random-walk error model for I_L . This is more realistic than white I_L noise given the correlated nature of error in modeling I_L . The sensitivity of orbit estimation using uncorrelated-error assumptions to the ionospheric frequency shift may thus be less than that to the corresponding range error.

DRVID (Equation (7)) data are themselves of no direct use for orbit determination, but they contain information about the ionospheric biases. Spacecraft and tropospheric effects, as well as other systematic errors common to pulse-delay and phase-delay measurement, cancel in the DRVID subtraction. DRVID is a measurement (with error from $(E_L - e_L)$) of the ionospheric Doppler correction. Summed DRVID data (SDRVID) measures the range correction (modulo an arbitrary constant bias for each pass). DRVID information can help validate ionospheric correction algorithms and models of ionospheric error.

The summed form of $DR \pm ID$ is most useful for the current purposes. The noise of $DR \pm ID$ measurements is dominated by that of the DR component, with correlations implied by its origin as successive differences of independent range measurements. Summing removes the effect of these correlations, if the resulting sequence is treated as biased. The correlation induced by summing the Doppler component is much smaller. In fact, the Dopplers may be *less* correlated in summed form, since the Doppler count is a coherent phase measurement (Reference 3). In addition, the Bent model for the ionospheric correction (used in the Goddard Trajectory Determination System (GTDS)) provides I_L , from which ΔI_L is calculated for Doppler correction. The comparison between real and modeled ionospheric corrections is thus more straightforward in summed DRVID than in the unsummed form.

Orbit determination accuracy benefits passively from the DRVID principle, since estimation processes implicitly compare the range and Doppler data. The sign opposition of the I_L terms in Equations (1) and (5) is effective whether or not the user deliberately exploits it. Under certain idealized conditions of symmetry in the treatment of the range and Doppler

measurement streams, there is automatically no effect of the ionosphere on orbit determination (except as it may affect data selection). These conditions are the following:

1. The ranges are converted into DR or the Dopplers are partially summed to SID.
2. If the latter, both a range bias and a Doppler-sum bias are solved for.
3. The weights of the range and SID (or DR and ID) are equal in the diagonal weight matrix.
4. The range- and Doppler-derived measurements are accepted and edited in matched pairs.

Under these conditions, a formal transformation of the range- and Doppler-derived measurements into their sum and difference ($DR \pm ID$ or their partial sums) leaves their covariance matrix diagonal. (This formal transformation is only a device of mathematical proof and need not be implemented in the numerical solution methods.) Equations (6) and (7) show that the normal equations then decouple into ionospheric and spacecraft sectors. Not only would ionospheric error have no effect on the orbit determination, but a large number of ionospheric variables (potentially as many as the number of observation pairs) may be solved for without impact, except possibly through editing, on the orbit determination sector. Enforcing conditions 1 through 4 is a way of achieving DRPID-only (or SDRPID-only) orbit estimation passively.

The above conditions (particularly the first) are not those under which orbit determination is normally performed (although the second alternative in condition 1 *should* be the norm if Doppler phase noise dominates frequency noise). Nor are these conditions optimal, because range noise is far greater than Doppler noise, even when the latter is summed. Furthermore, it may not be desirable to discard the range zero-set information by differencing or bias-solution. However, the above theorem shows that the measurement information already existing in standard two-way range and Doppler measurements is adequate to support the solution for multiple parameters of a flexible ionospheric model. If the DRPID data are considered to be the result of correcting the Doppler measurement ionospherically using a noisy DRVID-measured correction, then estimating a multiparameter ionospheric model in each pass is one way of smoothing out the influence of the range noise on the Doppler correction. The advantage of this is its seamless integration with existing estimation methodologies and its potential applicability to real-world nonsymmetric estimation.

TDRSS User

For TDRSS (including BRTS) applications, the pilot effects on the Doppler observation complicate the picture:

$$DRPID = \frac{1}{2} \Delta \left[R_L + T_L + \frac{1}{2} (e_L + E_L) + \frac{b}{2} (R_S + T_S + e_S) \right] \quad (8)$$

$$DRVID = \frac{1}{2} \Delta \left[I_L + \frac{1}{2} (E_L - e_L) - \frac{b}{2} (R_S + T_S + e_S) \right] \quad (9)$$

The pilot term (the term on the right-hand side of these equations that is multiplied by $b/2$) plays no different role in Equation (8) than in Equation (4) (with Equation (5)). TDRSS measurement analysis has always required a relay trajectory model. Orbit determination with DRPID measurements is qualitatively the same as with Doppler measurements, except that the ionospheric correction is unneeded, the noise is greater, and the pilot coefficient is half as big. DRPID (or SDRPID) orbit determination can still be implemented passively by enforcing conditions 1 through 4 (see above) for symmetric treatment of range and Doppler measurements; however, the following fifth condition must be added:

5. The variables affecting R_S (e.g., the TDRS state) are excluded from the state vector; otherwise orbit variables will be influenced by the (purely formal) DRVID sector (Equation (9)).

The use of DRVID as an ionospheric measurement is affected by the presence in the DRVID Equation (9) of the relay spacecraft degrees of freedom absent in Equation (7). For LEO DRVID, the time scales for variation of the ionospheric terms (10–1000 seconds) are much shorter than those of the pilot terms (fractions of a day). With a model of the TDRS trajectory, correction can be made for the effect of the pilot terms on what may still be regarded as an ionospheric measurement (with a new error source). Equations (1) through (9) apply to observed measurements (O), calculated measurements (C), and observed-minus-corrected (O-C) residuals in an estimation process. In GTDS differential correction (DC) processing, calculated TDRSS measurements take account of the pilot term using a relay trajectory model. The O-C version of Equation (9) has a pilot term coming only from *errors* in the relay trajectory and pilot models. DRVID analysis of O-C residuals is a convenient way of taking advantage of the pilot-loop modeling that is part of the DC processing of TDRSS observations.

The error in modeling the pilot term depends on the accuracy of the TDRS orbit model and the tropospheric delay model. Only the changing part of the error is significant. For LEO user passes that are not too long, an error estimate as an average range rate is appropriate, since these TDRS-associated quantities change slowly. The “wet” component (the most variable part) of the one-way

tropospheric delay can change as much as 5 centimeters in an hour (Reference 4) at zenith. Therefore, for a tracking contact of length τ , the buildup of tropospheric error in SDRVID is

$$\frac{1}{4}\delta T_s \lesssim \frac{1}{4} \cdot (0.05 \text{ meter/hour}) \cdot \tau \cdot (\sin E)^{-1} \cdot 2 \approx \tau \cdot (0.14 \text{ meter/hour}) \quad (10)$$

at elevations, E , around 10 degrees. The TDRS orbit uncertainty is dominated by the along-track and cross-track components, but the effect of these is reduced geometrically by a factor of the ratio of the TDRSS orbital radius to the Earth radius, making the effect of radial uncertainty comparable. Assuming a 50-meter uncertainty, the peak error is approximately

$$\frac{1}{4}\delta R_s \approx \frac{1}{4} \cdot (50 \text{ meters}) \cdot 2\pi \frac{\tau}{\tau_T} \cdot \frac{R_E}{R_T} \cdot 2 \cdot 2 \approx \tau \cdot (2 \text{ meters/hour}) \quad (11)$$

where τ_T is the TDRS orbital period (1 day), R_E is the Earth radius (6400 kilometers), and R_T is the TDRS orbital radius (42000 kilometers). One factor of 2 accounts for the addition of the radial error to the contribution of along-track and cross-track error and the other accounts for the round-trip. A somewhat smaller estimate is obtained from typical root-mean-square (RMS) BRTS residuals of less than 10 meters in the TDRS orbit solutions (e.g., Reference 5),

$$\frac{1}{4}\delta R_s \lesssim \frac{1}{4} \cdot (10 \text{ meters}) \cdot 2\pi \frac{\tau}{\tau_T} \lesssim \tau \cdot (0.7 \text{ meter/hour}) \quad (12)$$

Perhaps much of the orbit error in Equation (11) is in the direction to which R_s is insensitive. This is reasonable since local BRTS measurements (those for which the BRTS transponder is near the ground terminal antenna) account for half of the observations in the TDRS orbit estimation process. Thus, Equation (12) provides the more realistic error estimate, despite its inclusion of the S-band ionospheric error that should be nearly absent from the K-band pilot error. These error estimates must be multiplied by b to gauge their impact on measuring $I_l/2$. This brings the SA error to 3 meters per hour.

Bilateration Ranging Transponder System (BRTS)

A somewhat different analysis is required for DRVID analysis of BRTS tracking. Here, nothing is gained by eliminating the user degrees of freedom while leaving the relay degrees of freedom to be modeled—the two are the same. Using Equation (9) to investigate I_l is no better than using Equation (1). The accuracy of both analyses is limited by knowledge of TDRS-to-terminal nonionospheric delays, R_{sL} , T_{sL} , and E_{sL} . Modeling of the short and long loops is a single problem. Remote BRTS transponder tracking is not useful for DRVID analysis without simultaneous local-transponder or direct observations (through the K-band Telemetry, Tracking and Command (TT&C) channel at the Second TDRSS Ground Terminal (STGT)) to supply the TDRS-to-terminal range information.

Local BRTS measurements, however, present new possibilities for DRVID analysis with less pilot-loop error than TDRSS-user DRVID. The proximity of the tracked BRTS transponder to the ground terminal antenna guarantees that R_s and T_s are close to half of their long-path counterparts. Redefining ID for this case as

$$ID_B \equiv -\frac{c \Delta T}{2A + bA} D \quad (13)$$

yields

$$ID_B = \Delta r_B \quad (14)$$

with a revised phase-range, r_B , (ignoring the short-path K-band ionospheric effect, I_s) given by

$$r_B \equiv \frac{1}{2} \left[\begin{aligned} &(R_L + T_L + D_L + e_L) - \frac{2}{2+b} I_L + \dots \\ &+ \frac{2b}{2+b} (R_s - \frac{1}{2} R_L + T_s - \frac{1}{2} T_L + D_s - \frac{1}{2} D_L + e_s - \frac{1}{2} e_L) \end{aligned} \right] + C'_r \quad (15)$$

This reformulated phase range, as with the original user phase range, differs from the range measurement of Equation (1) by the constant multiplying the ionospheric effect, instrumental differences (e_L versus E_L), and a pilot term that now includes only the differences between the short path and half the long path.

DRVID is also redefined for this case so as to extract the one-way ionospheric effect from comparison of DR and ID_B as follows:

$$DRVID_B \equiv \frac{2+b}{4+b}(DR - ID_B) \\ = \frac{1}{2} \Delta \left[I_L + \frac{2+b}{4+b}(E_L - e_L) - \frac{2b}{4+b} \left(R_S - \frac{1}{2}R_L + T_S - \frac{1}{2}T_L + e_S - \frac{1}{2}e_L \right) \right] \quad (16)$$

DRPID does not benefit from or need any reformulation for local or remote BRTS tracking, but it does, of course, have a relationship to ID_B different from that to ID:

$$DRPID \equiv \frac{1}{2} \left[DR + \left(1 + \frac{1}{2}b \right) ID_B \right] \quad (17)$$

Pilot error for O-C analysis of DRVID for local BRTS tracking comes from lack of knowledge of the difference between the short path and half the long path. This is nonzero both because of the separation, δx_B , between the ground terminal and the BRTS transponder and because of the slight difference between the forward- and return-link portions of the long path. The former contribution is proportional to the TDRS angular uncertainty as seen from the ground site,

$$\frac{1}{2} \delta \left(R_S - \frac{1}{2}R_L \right) \lesssim \frac{1}{2} \cdot \frac{50 \text{ meters}}{R_T} \cdot \delta x_B \cdot 2 \lesssim 0.006 \text{ meter} \quad (18)$$

where the upper bound applies even for the 5-kilometer separation between the STGT (not used in the present work) and the BRTS site at the original White Sands Ground Terminal (WSGT). (Since there is no geometrical limitation to BRTS pass lengths, the assumption of short tracking contacts is inapplicable; therefore, the factor $2\pi \tau / \tau_T$ in Equations (10) through (12) is absent for calculation of the total variation over a TDRS orbit.) The latter effect is negligible ($\sim 10^{-4}$ meter) if typical RMS BRTS Doppler residuals (~ 0.010 hertz) are at all representative of knowledge of the TDRS orbit. The tropospheric refractive delay, per passage through the atmosphere, must be essentially the same for the long and short loops when the receive/transmit antenna and the BRTS transponder are as close together (0.6 kilometer (km)) as WSGT and the local BRTS site, WHSJ. For STGT and WHSJ, the possibility of meteorological differentials between the two sites exists. If, for example, the TDRS-to-BRTS legs pass through a spherical cloud of water vapor at 20°C (that the other legs miss) with a 1-inch peak rain capacity, the following DRVID error results:

$$\frac{1}{2} \delta \left(T_S - \frac{1}{2}T_L \right) \lesssim 0.15 \text{ meter} \quad (19)$$

based on a water-vapor refractivity of 87×10^6 and density of 15grams/meter³ at, for example, a 20-millibar partial pressure (86-percent humidity) (Reference 6). This entails about 3 hours worth of the zenith delay change, cited as a "not unusual" maximum rate by Reference 4, and so is presumably quite infrequent. These error estimates must be multiplied by $[4b/(2+b)]$ (about 0.7 for MA and 1.1 for SA) to gauge their impact on $I_L/2$.

Analysis Techniques

The O-C residuals were collected for a variety of tracking systems (USB (30-foot dish) and TDRSS), spacecraft (LEO and geosynchronous), and time periods, primarily in the last solar maximum timeframe (as shown in Table 1 given on the next page). All the TDRSS observations used WSGT. Residuals were calculated both without and with (except for TOPEX) ionospheric corrections derived from the Bent model with historical solar flux measurements. Tropospheric corrections were always applied. Doppler residuals were converted to ID (Equation (3)) and summed (to SID, i.e., the summed integrated Doppler). (The initial value of the partial sum was chosen so that the mean over each pass matched the mean range residual.) Comparison of the range residuals with the SID residuals was carried out graphically, for both ionospherically corrected and uncorrected residuals, and by subtraction as SDRVID.

Tracking data were obtained from archives of the FDF primary operational 60-byte database in the form of range (converted from raw light-delay time) and Doppler (converted from raw Doppler count) observations. Residuals against observation and trajectory models of a GTDS O-C run on the FDF IBM mainframe computers were captured to full 8-byte floating-point precision. Data on O, C, O-C, time, ionospheric correction, and validity flagging were downloaded to a DOS personal computer (PC), where they were analyzed and graphed using commercial plotting software, principally MATLAB. Full-precision capture was necessary (and sufficient) to reduce to insignificance the truncation error involved in summing long series of ID values. Some raw Doppler count data were analyzed to check that this procedure was accurate (to 10^{-8} cycles) for even the longest passes (5000 seconds).

Only standard operational techniques were employed for trajectory and observation modeling (except for the addition of ionospheric corrections). The desire was only to obtain residuals that were small enough to make interesting features visible in a plot, at the level of a few centimeters, without hiding physically interesting phenomena or introducing artifacts. The user spacecraft trajectory and observation modeling errors appear equally in range (R) and SID residuals and do not affect the comparison. This is not so for the TDRS degrees of freedom, because of their effect on the short pilot path. It would have been desirable to use special methods and solutions for the relay modeling, but this was not done due to time limitations. All relay orbits for TDRSS-user analysis were obtained from operational Permanent TDRS Orbit Files (PTOFs), except in the case of TOPEX, for which special orbit files were available (Reference 7). The pilot-tone error estimates given in the previous section reflect this decision.

Ionospheric corrections included the spacecraft-to-spacecraft legs (TDRSS-user tracking) and the S-band ground-to-space legs (BRTS and GN). These were calculated by a GTDS enhancement called GATFTR, which adds the calculation of the spacecraft-to-spacecraft legs using Gaussian integration, as described in Reference 8.

The source of user spacecraft orbital elements varied in this study (see Table 1, column 7). The original intention was to use elements from operational solutions, and this was followed for those spacecraft for which Table 1 describes the elements source as Ops. In three cases (indicated by Corr DC in the Elements Source column of Table 1), orbital elements were obtained from special DCs employing Bent-model ionospheric corrections. Special DC results (ionospherically uncorrected), which were already available for TOPEX (Reference 6), were used for this spacecraft, as noted in Table 1.

Ideally, the definition of a tracking pass, for purposes of this analysis, should be a period of continuous coherency in two-way range and Doppler tracking. In general, therefore, the interval between two successive Doppler observations should be equal to the Doppler count interval of the latter, usually 10 seconds. However, interpolation of a few Doppler residuals to cover a

Table 1. Spacecraft and Tracking Periods for DRVID Analysis

Spacecraft *	Tracking			Orbit			10.7-Centimeter Solar Flux (10^{-22} watts/meter ² /hertz)	
	Dates	Source	Passes	Semimajor Axis (km)	Inclination (degrees)	Elements Source **	365-Day Mean	Daily
TDRS-1	05/15/89	BRTS	1	42164	3.7	Corr DC	214	183
TDRS-1	12/01-12/02/91	BRTS	3	42166	5.9	Ops	193	172
TDRS-3	10/08/91	DS17/46	6	42054	0.2	Corr DC	201	179
ERBS	10/02/91	BDA3	1	6966	57.0	Corr DC	201	221
HST	10/18/91	TDRSS	11	6984	28.5	Ops	198	158
GRO	10/18/91	TDRSS	8	6816	28.5	Ops	198	158
TOPEX	10/13-10/15/92	TDRSS	20	7721	66.0	Uncr DC	131	106

* ERBS = Earth Radiation Budget Satellite; HST = Hubble Space Telescope; GRO = Gamma Ray Observatory; TOPEX = Ocean Topography Experiment

** Ops = Operational solution elements; Corr DC = ionospherically corrected DC elements; Uncr DC = ionospherically uncorrected DC elements

brief period of loss of Doppler coherency was employed in a few cases. For the very shortest gaps (30 seconds or less, as in TOPEX passes 7 and 13 and in GRO pass 5), residuals were simply zeroed. To cover gaps of 99 and 110 seconds in two long TDRS-1 passes, polynomials were fitted to residuals on either side of the gaps, and the fit values were used inside the gaps. In all cases, the number of interpolated residuals was sufficiently small that any error would have small visible impact on the SID residual plot for the pass.

Results

DRVID Pass Analysis

Table 2 summarizes the results for SDRVID residuals corrected (column 6) and uncorrected (column 7) by Bent-model ionospheric corrections. The correlation coefficient between the ionospherically uncorrected SDRVID residuals and the Bent

model expectation (for $I_L/2$) is given in column 8. High-frequency noise amplitude is estimated for corrected SDRVID residuals by piecewise polynomial fitting using degrees up to 15 with two segments per pass (column 9). The Bent-model relief (column 10) is defined as the difference between the maximum and minimum values of the modeled $I_L/2$. It is a measure of how distinctly the ionosphere is predicted to be visible in DRVID.

Since reproducing 50 plots of R and SID and 50 of SDRVID in this paper is impractical, a Bent model score, subjectively summarizing the general agreement between the plots and the expectations of the Bent model, is assigned in the last column of this table. The meaning of these scores is as follows:

- A = reasonable success, qualitatively and quantitatively
- B = at least some features qualitatively reproduced
- C = success; of marginal significance (ionospheric behavior not strong)
- D = ionospheric behavior insignificant relative to uncertainties
- E = failure; of marginal significance (ionospheric behavior not strong)
- F = qualitative and quantitative failure of Bent model

Figure 1 summarizes some of the results presented in Table 2. The difference between the RMSs of the uncorrected and corrected SDRVID residuals, respectively, is plotted against the Bent-model relief. The straight line shows the relationship between these two quantities that would hold for I_L linear versus time. The success of the Bent model is mixed. The ionospheric model is more successful, in general, the stronger the ionospheric effect is expected to be. In 7 of 10 passes with 2 meters or more of ionospheric relief, the Bent model improves SDRVID residuals, while it degrades them significantly in only one.

The results for each spacecraft are discussed below. Figures 2 through 13 cited in these discussions are given at the end of this Results section.

Hubble Space Telescope (HST) Results

The main emphasis in this work was on TDRSS-user tracking; the HST passes, which are MA with substantial ionospheric effects, give the best examples of this. Figures 2 and 3 show the DRVID comparisons for the fifth HST pass. The plot of R and SID residuals given in Figure 2 clearly shows the mirror image behavior expected from ionospheric transients, most strongly in the uncorrected data (compare range (+) with SID (solid line)). The persistence of a smaller amount of mirror image discrepancy in the corrected data (compare range (o) to SID (dashed line)) shows the imperfect effectiveness of Bent-model correction at removing ionospheric effects. Recall that the arbitrary constant in the definition of SID has been adjusted to null out the mean difference with R. The adjustment of the constant was performed independently for corrected and uncorrected data. The comparison of the uncorrected SDRVID residuals in Figure 3 (+) with the Bent-model for $I_L/2$ (biased to zero mean for comparison with SDRVID and plotted as a solid line) displays this model's success until the end of the pass, where it plateaus spuriously and then fails to reproduce the largest effects. The differences between these two equal the corrected SDRVID residuals (shown as o in Figure 3), which are therefore not reduced quite to zero, especially near the end of the pass. This pass exemplifies the score of A for the Bent model—good, but not great, agreement.

The third HST pass (Figures 4 and 5) exemplifies its B score. The Bent model agrees qualitatively with the uncorrected SDRVID residuals, correctly showing large increases at the wings, but undercorrects the beginning of the pass while overcorrecting the end. There is only a modest improvement in the RMS of the corrected SDRVID residuals.

The zigzags (covering up to 2 meters and 300 seconds) in both sets of SDRVID residuals in Figure 5 are, of course, absent from the Bent model. Examination of Figure 4 shows that these zigzags are present only in the range data and not in the Doppler (down to about 3 percent of the expected magnitude). They are therefore not ionospheric phenomena, which would cause mirror-image features in both R and SID. Neither are they from user spacecraft motion or modeling, which would produce parallel features in both R and SID. Nor are they solely short-path effects, which would appear in Doppler measurements, not ranges. Since this is an MA pass, with the ratio $b = -0.93$, the common effects of the TDRS-to-ground-terminal range on the short and long paths cancel down to the 7-percent level in Doppler but not in range observations. A likely cause would be one that affects only the TDRS range to ground (although 3-percent rather than 7-percent, attenuation is needed). TDRS spacecraft motion would likely affect both the range to the ground and to the user. The zigzags are too large to be a tropospheric effect or a ground antenna motion effect. These zigzags are seen only in this pass and remain unexplained, but they are certainly not ionospheric in origin.

Table 2. SDRVID Analysis Results

Pass ID	Tracking Source	Start Time (UTC)*	Elapsed Time (seconds)	Observation Count	Uncorrected RMS (meters)	Corrected RMS (meters)	Correlation With Bent Model	Noise Estimate (meters)	Bent Model Relief (meters)	Bent Model Score
TDRS-1 1989										
1	MA	16:45:10	6290	608	0.358	0.561	-0.44	0.23	1.27	E
TDRS-1 1991										
1	MA	05:09:40	1219	114	0.301	0.297	0.15	0.28	0.16	D
2	MA	12:45:40	2490	250	0.273	0.311	-0.16	0.25	0.38	D
3	MA	27:14:40	2480	249	0.527	0.410	0.80	0.28	0.54	C
All				613	0.400	0.352				
TDRS-3 1991										
1	DS17	06:06:00	4380	439	0.480	0.493	-0.03	0.48	0.35	D
2	DS46	07:21:50	3130	314	0.353	0.374	0.11	0.35	0.58	E
3	DS17	08:16:30	3450	346	0.456	0.455	0.05	0.44	0.04	D
4	DS46	09:16:50	1930	194	0.415	0.414	0.09	0.43	0.21	D
5	DS17	09:51:30	23080	2307	1.103	1.021	0.90	0.46	6.53	B
6	DS17	17:03:30	2250	226	0.556	0.486	0.49	0.44	1.01	C
All				3826	0.903	0.842				
ERBS 1991										
1	BDA3	16:32:10	500	51	2.904	1.140	0.92	0.66	9.22	A
GRO 1991										
1	SA	01:17:30	1100	111	7.274	2.856	0.95	0.15	24.17	A
2	SA	04:36:20	1160	117	1.980	2.024	0.25	0.21	3.58	B
3	SA	07:34:00	1660	167	1.466	0.935	0.92	0.24	2.67	B
4	SA	10:52:50	1670	168	3.756	1.886	0.96	0.27	8.47	B
5	SA	13:25:10	630	64	0.780	0.643	0.66	0.25	0.67	F
6	SA	15:53:30	1640	165	0.712	0.432	0.81	0.23	1.68	A
7	SA	19:49:20	1590	160	0.969	1.662	0.35	0.27	7.65	F
8	SA	21:41:20	1050	106	1.161	1.122	0.33	0.22	1.78	F
All				1058	2.982	1.610				
HST 1991										
1	MA	00:46:20	820	83	0.392	1.075	-0.89	0.09	1.91	F
2	MA	02:27:50	830	84	1.362	0.758	0.85	0.09	5.65	B
3	MA	06:33:10	2530	254	1.046	0.640	0.81	0.12	5.78	B
4	MA	08:32:00	840	85	0.244	0.223	0.46	0.13	0.26	D
5	MA	10:02:10	2570	258	2.110	0.609	0.96	0.12	6.44	A
6	MA	12:01:00	490	50	0.356	0.219	0.88	0.13	1.25	A
7	MA	13:51:50	1010	102	0.844	0.877	-0.08	0.12	0.71	F
8	MA	15:22:50	840	85	0.473	0.432	0.46	0.14	1.27	B
9	MA	18:02:50	830	84	0.157	0.133	0.67	0.08	0.56	C
10	MA	19:45:00	1340	135	0.250	0.226	0.46	0.10	0.67	C
11	MA	21:53:00	420	43	0.403	0.471	-0.64	0.12	0.37	E
All				1263	1.163	0.603				
TOPEX 1992										
1	SA	00:46:30	2300	231	0.303			0.22		D
2	SA	03:01:40	1690	170	0.318			0.22		D
3	SA	04:59:30	2300	231	0.253			0.21		D
4	SA	06:57:30	2300	231	0.242			0.23		D
5	SA	09:10:30	2240	225	0.269			0.21		D
6	SA	10:51:40	2290	230	0.325			0.21		D
7	MA	12:25:10	2260	225	0.222			0.11		D
8	MA	14:29:30	2180	219	0.148			0.06		D
9	SA	17:16:30	2300	231	0.325			0.28		D
10	MA	18:21:30	2300	231	0.113			0.07		D
11	SA	20:34:30	1460	147	0.276			0.25		D
12	SA	22:21:10	2200	221	0.307			0.27		D
13	SA	27:25:40	1690	169	0.272			0.23		D
14	SA	29:22:30	2300	231	0.266			0.24		D
15	SA	31:21:40	2290	230	0.308			0.27		D
16	SA	33:33:30	2300	231	0.333			0.28		D
17	SA	35:22:30	2300	231	0.259			0.26		D
18	MA	36:50:20	1760	177	0.154			0.06		D
19	MA	38:51:10	2320	233	0.169			0.12		D
20	MA	63:14:20	1970	198	0.140			0.08		D
All				4292	0.259					

* UTC = coordinated universal time

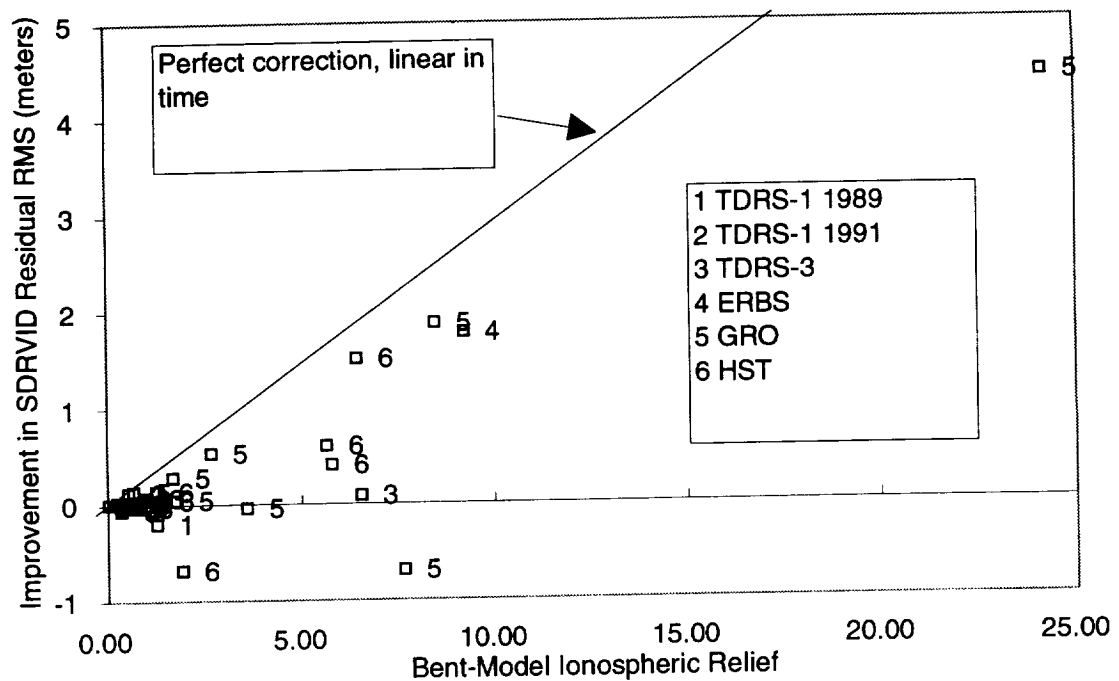


Figure 1. Improvement in RMS Residuals of SDRVID Due to Ionospheric Correction by the Bent Model

The first HST pass exemplifies its F score for the ionospheric model. Table 2 shows corrections tripling the RMS residual of SDRVID, despite a moderate amount of Bent-model relief. The SDRVID data of Figure 6 show why: the model ionospheric corrections decline by almost 2 meters while the measurements increase by almost a meter, for a 3-meter discrepancy. Pilot loop error can account for perhaps a tenth of this (Equation (12)). The Bent model is entirely wrong for this pass. (The plot of R and SID for this pass is omitted since it is unrevealing.)

Gamma Ray Observatory (GRO) Results

Because the GRO passes are all SA, somewhat more caution is needed in interpreting them because potential pilot errors may exceed 3 meters per hour. For example, Figure 7 for the second GRO pass shows the expected mirror-image discrepancies between R and SID not to be at all ameliorated by ionospheric correction. The plot of SDRVID for the pass (Figure 8) displays measured ionospheric features that are present in the Bent model but not quantitatively reproduced. Pilot loop errors at the 3-meters-per-hour level, as indicated by Equation (12) for SA, would not remove the discrepancy, but 25 meters per hour (in the central section only) would help. This would require 24-hour TDRS orbit error levels in the vicinity of 120 meters (along-track or cross-track) or 20 meters (radial), somewhat larger than typical.

The first GRO pass (Figure 9), on the other hand, provides a significant success for the SDRVID method, as well as for the Bent model, which predicts the one-way ionospheric delay to vary from 3.7 meters to 27.9 meters during the pass. At least 24.6 meters of delay at the end of the pass is confirmed by the SDRVID measurements, since the effect must be positive at the beginning of the pass. This includes TDRS line-of-sight elevations down to -3.6 degrees (relative to the local GRO horizontal plane). Even with a cutoff at $+5$ degrees elevation, 13.1 meters of delay are predicted at the end of the pass and at least 17.1 meters are observed. The RMS SDRVID residual is reduced from over 7 to under 3 meters, despite the model's imperfections in not ramping up soon enough or fast enough. This is one of few passes where unsummed DRVID measurements are significant and large. The average two-way Doppler ionospheric effect over a 200-second period (at the relatively high elevations of 15 to 26 degrees) is here *measured* at 0.58 ± 0.08 hertz (3.8 ± 0.5 centimeters per second). (The 3σ error estimates assume 1σ SDRVID noise of 0.25 meters.) Still higher rates are seen at negative elevations.

Ocean Topography Experiment (TOPEX) Results

The TOPEX results are generally uninformative, given the low levels of variation in the ionospheric delay both expected and observed. TOPEX tracking at this time was evidently geometrically selected to avoid significant ionospheric effects, and solar activity had declined from its peak. The last pass shows a half-meter step function (rise time about one minute) in the range residuals accompanied by a coincident Doppler peak with no more than 10 percent of the expected magnitude.

Earth Radiation Budget Satellite (ERBS) Results

The sole GN pass analyzed for a LEO spacecraft, ERBS, is another success (Figure 10) for the Bent model (this time applied to the ground-to-space line of sight). The fit of SDRVID to the model is excellent and the corrected residuals are uniformly small. As for all ground tracking of LEO spacecraft, the time variation of the correction is largely geometrically determined, while geophysical variation is often important in TDRSS passes for LEO users. A geometrical “cosec model”, proportional to the cosecant of the elevation of the line of sight at the point where it attains 300 km altitude, is plotted in Figure 10 to illustrate this point. (The cosec model is normalized to the Bent model at their common minimum.)

Tracking and Data Relay Satellite (TDRS) Results

The success of the ERBS GN analysis makes the unsatisfactory results displayed (Figure 11) for the fifth TDRS-3 pass puzzling, in contrast. The ionospheric correction for geosynchronous spacecraft varies chiefly due to change of the ionospheric state, not due to geometry as for LEO spacecraft. Long passes are therefore needed to demonstrate the DRVID effect. This is really the only geosynchronous spacecraft pass collected that was long enough (over 6 hours) to accumulate major ionospheric variation. Nine-point averages of SDRVID residuals are plotted to reduce clutter and noise. The Bent model correction is too variable by a factor of two in this pass. In fact, one-half of the Bent model (dashed line in Figure 11) is an excellent fit to the data, but this is apparently coincidental. Strenuous, but futile, efforts were made to locate a factor of 2 error in our analysis of this pass. The Bent model implementation used here is, moreover, exactly the same one as produced the success for ERBS.

Given the disappointing results for TDRS-3 above, it is not surprising that the analysis of the necessarily shorter BRTS passes was not a great success. Only a single pass was located as long as the 1.75-hour TDRS-1 event in 1989 (Figure 12). Other shorter passes (see Table 2) did not display enough ionospheric variation for definitive analysis. Although the Bent model dictates that the 1989 pass should have participated in the steep morning (local time) increase in ionospheric effect (Figure 13), the measurements suggest that the diurnal peak had already passed.

Conclusions

Mirror-image transients in range and SID residuals for LEO TDRSS users (e.g., Figures 2 and 7) are clearly related to the Bent model for the ionospheric effect (e.g., Figures 3 and 8) qualitatively and sometimes quantitatively. This demonstrates the existence of the DRVID effect in TDRSS tracking. More importantly, it demonstrates that quantitative measurements of ionospheric effects can be synthesized from ordinary TDRSS coherent tracking. The noise level for measurement of variation in one-way ionospheric range corruption is one-half the range noise, i.e., 6 to 14 centimeters for MA and 15 to 28 centimeters for SA (see Table 2). Systematic errors are 1 to 2 meters per hour of pass length (Equations (11) and (12)) for MA and 5 times that level for SA, but they can be reduced if special care is employed in TDRS orbit modeling. The potential utility in critical evaluation of existing and future ionospheric correction models is evident.

To make full use of this potential, certain transient behaviors in range data that are not reflected in Doppler observations must be understood. These have been observed in the GRO and TOPEX MA ranges at time scales of 1 second to a few hundred seconds and amplitudes of 0.5 to 2 meters. They are caused neither by the ionosphere nor by user spacecraft motion. Even if these transients have a purely instrumental origin, a greater understanding of them will aid in the interpretation of DRVID comparisons.

Comparison of R and SID residuals is also a potential tracking data quality evaluation tool. The range transients mentioned above, for example, are too small to have been considered significant without the SID comparison.

Quite large ionospheric corruption of tracking measurements has been observed (not predicted or modeled) in this study to have occurred during the last solar maximum. Range effects were at least 24.6 meters, over 17 meters of which occurred above 5 degrees in TDRS elevation in a GRO pass. Average ionospheric frequency shifts of 0.6 hertz over a 200-second period at elevations above 15 degrees were also observed in this pass.

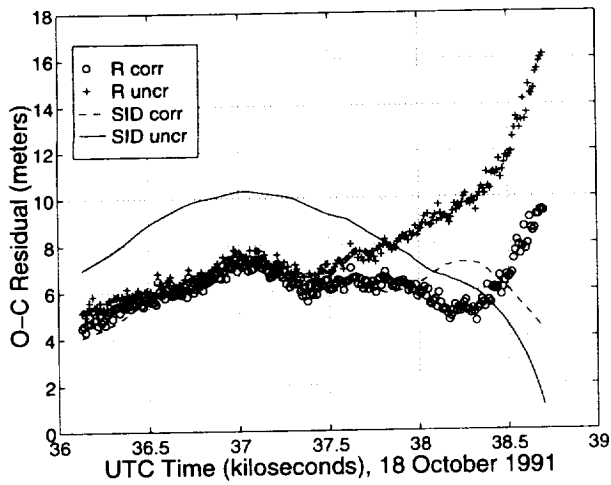


Figure 2. Range and SID Residuals for the Fifth HST Pass

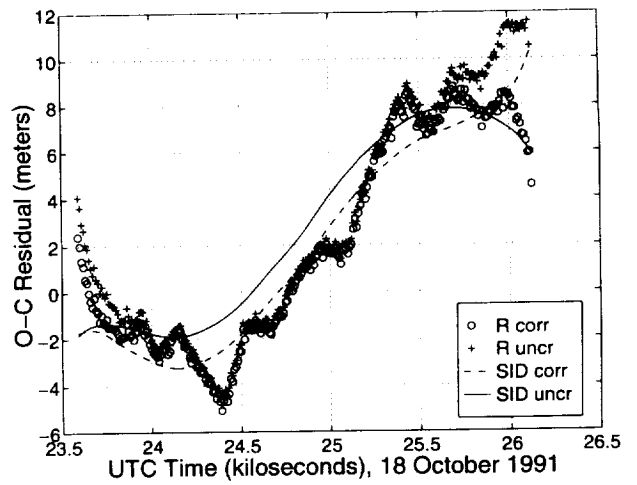


Figure 4. Range and SID Residuals for the Third HST Pass

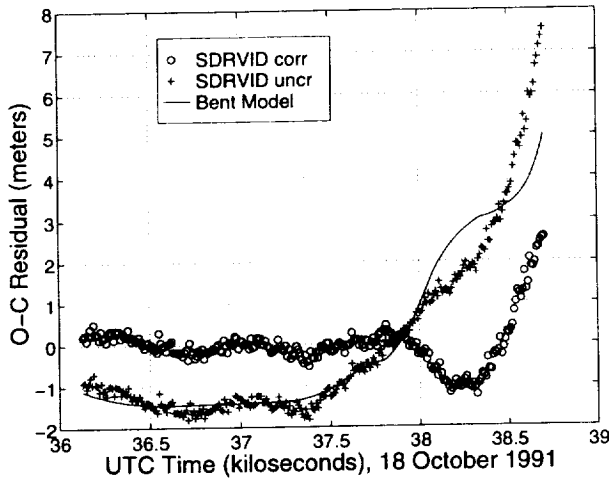


Figure 3. SDRVID Residuals for the Fifth HST Pass

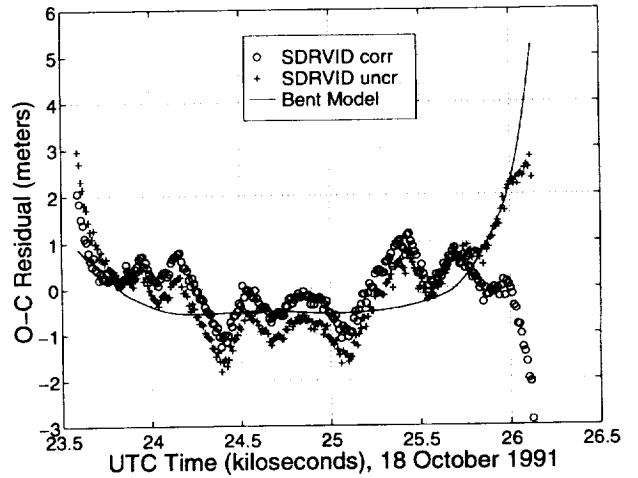


Figure 5. SDRVID Residuals for the Third HST Pass

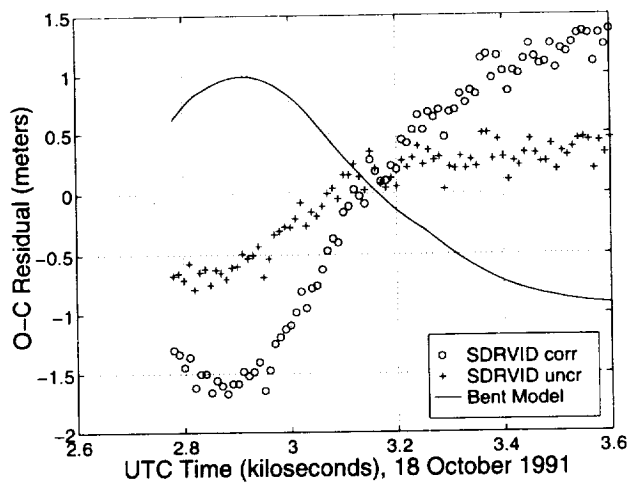


Figure 6. SDRVID Residuals for the First HST Pass

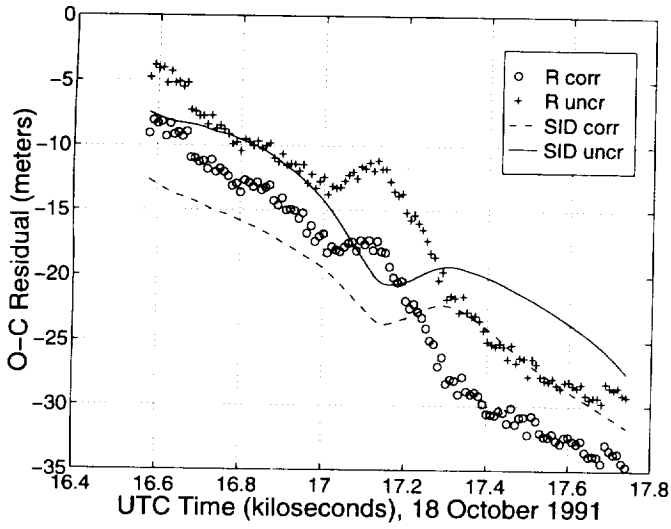


Figure 7. Range and SID Residuals for the Second GRO Pass

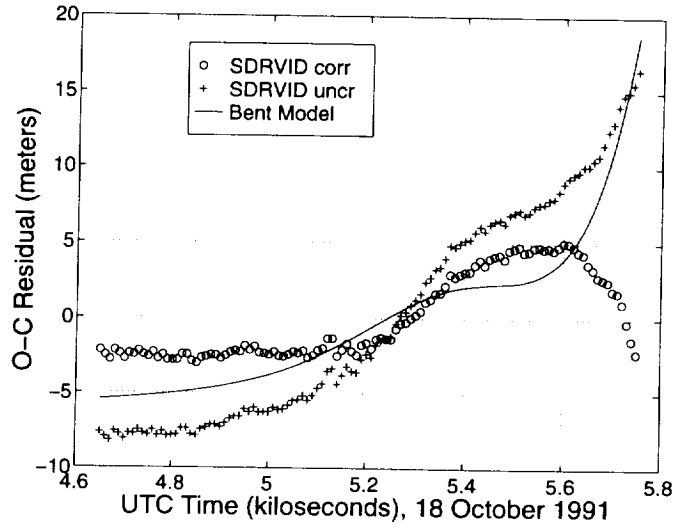


Figure 9. SDRVID Residuals for the First GRO Pass

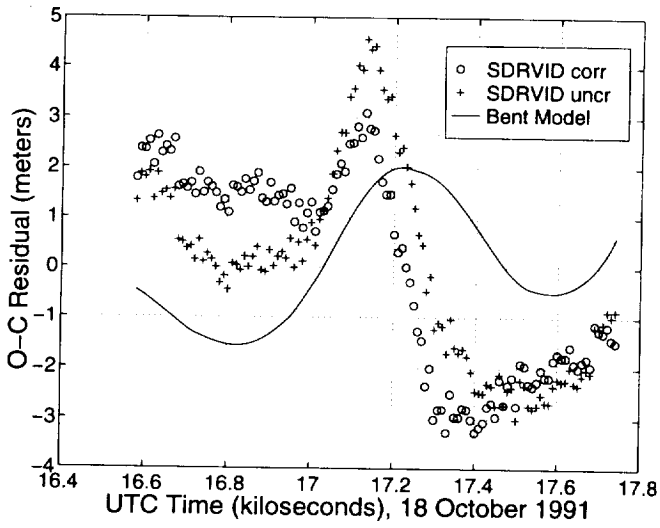


Figure 8. SDRVID Residuals for the Second GRO Pass

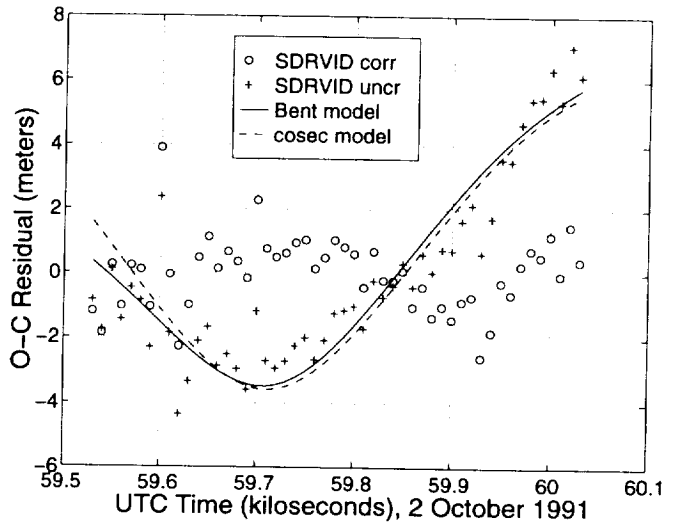


Figure 10. SDRVID Residuals for the ERBS Pass

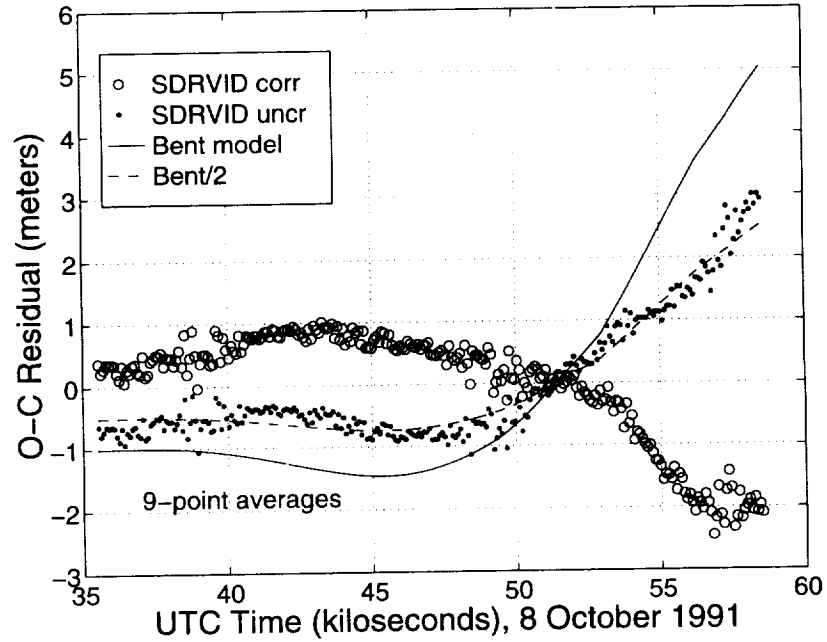


Figure 11. Nine-Point Average SDRVID Residuals for the Fifth TDRS-3 Pass

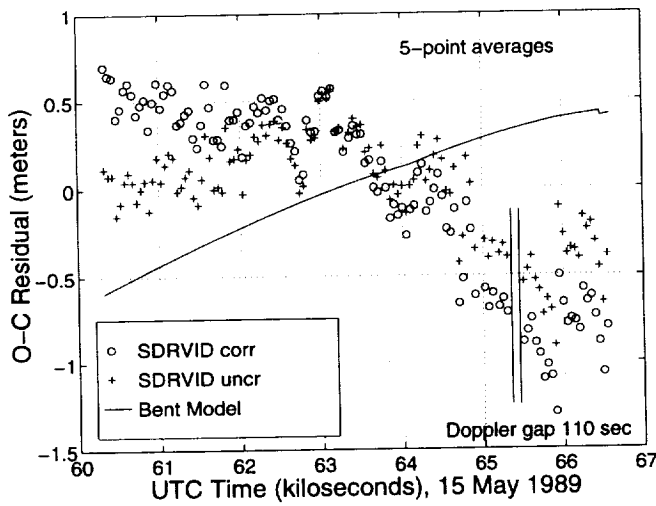


Figure 12. Five-Point Average SDRVID Residuals for the 1989 TDRS-1 Pass

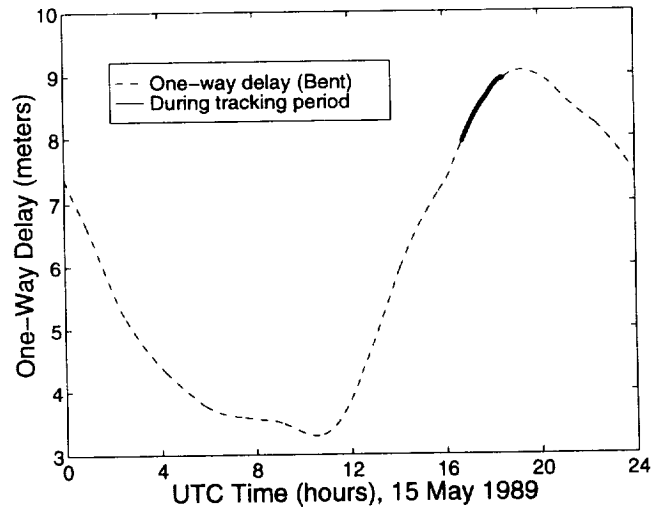


Figure 13. Diurnal Dependence of One-Way Ionospheric Range delay in the Bent Model

Ionospheric corrections for observations of geosynchronous spacecraft change slowly as does the ionosphere itself. Very long tracking passes are therefore required for significant observation of these changes using DRVID. In the only two passes (one a GN and one a BRTS pass) where obviously significant changes occurred, the Bent model performed poorly. It is puzzling how the same correction algorithm can produce accurate variations with geometry at a particular time of day (as the Bent model for USB tracking did for our ERBS pass) and yet overestimate by 100 percent the diurnal time variation at a particular geometry (as it did for the TDRS-3 pass), unless the former success is coincidental.

It appears that useful DRVID analysis of TDRS spacecraft will require specially requested long tracking passes. One or a few 24-hour White Sands BRTS passes (for each of TDRS-East and TDRS-West) would reveal much about ionospheric modeling of these crucial ground-to-space links. Since the night-time ionosphere is relatively quiescent, DRVID measurement of a complete cycle of the diurnal ionospheric delay variations translates into knowledge of the delay with relatively little bias uncertainty. Simultaneous continuous tracking of the remote transponders would permit the same sort of information to be extracted for those paths. The burden on the TDRSS, monopolizing one or even two (of only three) forward S-band services per TDRS for a whole day, would be considerable.

DRPID data is unbiased by the ionosphere and presents possibilities for self-correcting orbit determination with little or no dependence on ionospheric modeling. Possible tracking selections for LEO user orbit determination include DRPID-only, SDRPID-only, and SDRPID + Doppler. The first of these is of interest primarily because it can be implemented very easily in existing software systems for evaluation. TDRS orbit determination with TT&C tracking plus remote-transponder DRPID or SDRPID is a remote possibility that should also be evaluated.

It is possible that the best way to use the DRVID principle in orbit estimation is to solve for several ionospheric correction parameters per pass while still using conventional range and Doppler observations. The influence of these parameters under least-squares minimization will tend to resolve the conflicts between range and Doppler information that are caused by the opposite signs of I_L in Equations (1) and (4). Perhaps a set of phenomenological ionospheric correction models can be found that covers all the various geometrical relationships between the line of sight and the ionosphere (vertically moving, horizontally moving, and stationary). If the number of ionospheric parameters per pass can, with fidelity to the DR-ID data, be kept small relative to the number of observations, what is effectively DRPID or SDRPID orbit determination need not import overwhelming range-difference noise onto the Doppler dataset. If this set of models furthermore realistically correlates the time-dependent shape of the ionospheric correction with its zero point, as is possible for nonlinear models that (like the real ionosphere) yield positive-definite delays, then even some of the undifferenced absolute range information may be preserved.

References

1. P. F. MacDoran, "A First-Principles Derivation of the Differenced Range Versus Integrated Doppler (DRVID) Charged-Particle Calibration Method," *Space Programs Summary 37-62*, Vol. II, March 1970.
2. J. Teles, Computer Sciences Corporation, private communication, September 1994.
3. Goddard Space Flight Center, X-572-80-26, *Tracking and Data Relay Satellite System (TDRSS) Range and Doppler Tracking System Observation Measurement and Modeling*, P. B. Phung, V. S. Guedeney, and J. Teles, September 1980.
4. T. P. Yunck, "Coping With the Atmosphere and Ionosphere in Precise Satellite and Ground Positioning," *Environmental Effects on Spacecraft Positioning and Trajectories*, IUGG Geophysical Monograph 73, Vienna, 1991.
5. Computer Sciences Corporation, 554-FDD-91/097, SEAS(550)/IM-91/034(51.443), *Tracking and Data Relay Satellite (TDRS) Orbit Determination With Amended Ionospheric Refraction Corrections*, M. Radomski, May 1991.
6. E. K. Smith and S. Weintraub, "The Constants in the Equation of Atmospheric Refractive Index at Radio Frequencies," *Proceedings of the I.R.E.*, Volume 41, pp. 1035-1037, August 1953.
7. C. E. Doll, G. D. Mistretta, R. C. Hart, D. H. Oza, D. T. Bolvin, C. M. Cox, M. Nemesure, D. J. Niklewski, and M. V. Samii, "Improved Solution Accuracy for TDRSS-Based TOPEX/Poseidon Orbit Determination," *Proceedings of the Flight Mechanics/Estimation Theory Symposium 1994*, NASA Conference Publication 3265, May 1994.
8. Computer Sciences Corporation, CSC/TM-87/6710, Analysis Report 87005, "A Model for Assessing the Tracking Measurement Refraction Effect on TDRSS User Orbit Determination," *Operational Orbit Techniques Compendium of Analysis Reports*, M. Radomski, December 1987.

